Journal of Materials Chemistry A

RSC Publishing

COMMUNICATION

View Article Online
View Journal | View Issue



Cite this: *J. Mater. Chem. A*, 2013, **1**, 8101

Received 30th April 2013
Accepted 29th May 2013

DOI: 10.1039/c3ta11694h

www.rsc.org/MaterialsA

# Microwave-assisted deposition of metal sulfide/oxide nanocrystals onto a 3D hierarchical flower-like $TiO_2$ nanostructure with improved photocatalytic activity†

Liyuan Mao,[a] Yanrong Wang,[a] Yijun Zhong,[a] Jiqiang Ning[b] and Yong Hu*[a]

**An effective and general microwave-assisted strategy has been developed for deposition of monodisperse metal sulfide/oxide nanocrystals on the surface of a type of 3D hierarchical flower-like nanostructure to form $TiO_2$-based metal sulfide/oxide hetero-nanostructures. We choose the as-prepared $TiO_2$–CdS hetero-nanostructure as an example, which exhibits obviously enhanced photocatalytic activity for the photodegradation of methyl orange (MO) compared with $TiO_2$ nanoflowers, P25 and pure CdS under visible-light irradiation.**

During the past few decades, many research efforts have been concentrated on the environmental application of semiconductor photocatalysts for water and air purification.[1–5] Titanium oxide ($TiO_2$), as an important functional material, has attracted tremendous attention in both fundamental studies and practical applications due to its high photocatalytic activity, low-cost, non-toxicity, photostability, and unique electronic and optical properties.[6–11] However, its development is still hindered by the bottleneck of poor quantum yield caused by the rapid recombination of photogenerated electrons and holes and its broad bandgap responding only to UV light. To overcome these obstacles, the photocatalytic activity of $TiO_2$ can be improved through integrating other active materials to form $TiO_2$-based nanocomposites, such as $TiO_2$–semiconductors,[12,13] $TiO_2$–noble-metals,[14,15] $TiO_2$–carbon,[16,17] *etc.* In particular, $TiO_2$-based semiconductor hetero-nanostructures have received extensive research efforts owing to their enhanced photocatalytic activity by extending the photoresponding range and increasing the electron–hole pairs separation.[18,19]

Very recently, three-dimensional (3D) hierarchical nanostructures have been proved to be one of the most important factors directly influencing the photocatalytic activity of $TiO_2$-based photocatalysts,[20–22] which exhibit superior photocatalytic activity compared with other lower-dimensional structures. Because hierarchical nanostructures possess good light-scattering properties, they are expected to provide more efficient light harvesting and higher specific surface area than their low-dimensional counterparts.[23–25] Meanwhile, such 3D hierarchical structures with a size on the micron-scale are in favour of carrier separation and recycling in practical applications.[26] Due to the high concentration of hydroxyl groups on the surface, $TiO_2$ is an ideal supporting material for the adsorption of metal ions.[27] Based on these advantages, $TiO_2$ hierarchical nanostructures are good candidates for excellent support materials coupling with other semiconductor nanocrystals to improve photocatalysis performance.

In this work, we demonstrate an effective and general strategy developed for the deposition of monodisperse CdS, ZnS, ZnO or $CeO_2$ nanocrystals on the surface of a 3D hierarchical flower-like nanostructure to form $TiO_2$-based metal sulfide/oxide hetero-nanostructures *via* a rapid microwave-assisted method using $TiO_2$ nanoflowers and different metal salts as starting materials. Microwave irradiation is an attractive and facile method for rapid synthesis of nanocrystals with a small particle size, narrow size distribution, and high purity.[28] In the present synthesis strategy, 3D hierarchical flower-like $TiO_2$ nanostructures were first prepared *via* a facile one-pot solvothermal approach followed by an annealing treatment, and then acted as the supporting materials in the following microwave-assisted reaction process. After absorbing metal ions on the surface of $TiO_2$ nanoflowers in the presence of thioacetamide (TAA) or hexamethylenetetramine (HMT), the mixture was placed in a microwave refluxing system and irradiated at 300 W for 30 min to obtain $TiO_2$-based metal sulfide/oxide hetero-nanostructures, through which a conformal nanocrystal layer was deposited onto $TiO_2$ nanoflowers retaining the uniformity of the original $TiO_2$ morphology. A variety of

[a]*Key Laboratory of the Ministry of Education for Advanced Catalysis Materials, Institute of Physical Chemistry, Zhejiang Normal University, Jinhua, 321004, P. R. China. E-mail: yonghu@zjnu.edu.cn*

[b]*Department of Physics, HKU-CAS Joint Laboratory on New Materials, The University of Hong Kong, Pokfulam Road, Hong Kong, P. R. China*

† Electronic supplementary information (ESI) available: Details of the synthesis method and complementary XRD, SEM and element mapping analysis. See DOI: 10.1039/c3ta11694h

nanocrystals, including CdS, ZnS, ZnO, and $CeO_2$, were deposited to prepare the $TiO_2$-based heterostructures. As a proof-of-concept demonstration of the functional properties of these hierarchical heterostructures, we choose the as-prepared $TiO_2$–CdS hetero-nanostructure as an example to exhibit the obviously enhanced photocatalytic activity for the photodegradation of methyl orange (MO) compared with $TiO_2$ nanoflowers, P25 and pure CdS under visible-light irradiation.

The crystallographic structure and phase purity of the as-obtained 3D hierarchical flower-like $TiO_2$ nanostructure synthesized with 35 mL of ethylene glycol (EG) and 5 mL of water in the reaction solution, and different $TiO_2$-based hetero-nanostructures are first confirmed by powder X-ray diffraction (XRD) analysis, as shown in Fig. 1. For $TiO_2$ nanoflowers, all the diffraction peaks marked by circles can be well indexed to the pure anatase phase of $TiO_2$ (JCPDS card no. 21-1272; $a = 3.785$ Å and $c = 9.513$ Å). For different $TiO_2$-based hierarchical heterostructures, in addition to the obvious $TiO_2$ diffraction peaks, the other peaks can be well assigned to hexagonal phase CdS (JCPDF card no. 41-1049), sphalerite-phase ZnS (JCPDS card no. 05-0566), hexagonal phase ZnO (JCPDS card no. 36-1451) and cubic $CeO_2$ (JCPDS no. 34-0394), respectively. No additional peaks were detected, indicating the high purity of the resultant samples.

The morphology and structure of the as-obtained $TiO_2$ nanoflowers and the different $TiO_2$-based hetero-nanostructures are further characterized by scanning electron microscopy (SEM) and transmission electron microscopy (TEM). A panoramic view of the as-prepared $TiO_2$ product (Fig. 2a) reveals that the sample is entirely composed of uniform hierarchical flower-like microstructures with an average size of 1.5 μm. Fig. 2b shows that the flower-like microstructure is made up of a large quantity of nanowires about 20–30 nm in diameter. Moreover, the surface of $TiO_2$ is relatively smooth without secondary nanostructures, indicating a high uniformity of the hierarchical flower-like morphology. It was found that the relative amount of ethylene glycol (EG) and water in the mixed solvent is an important parameter that greatly affects the morphology of the $TiO_2$ nanoflowers obtained from the solvothermal processes. To investigate this effect on the product morphology, a series of experiments were carried out by varying the EG amount in the reaction system while keeping other conditions unchanged (Fig. S1, see the ESI†). From these results, it can be seen that further decrease of the amount of EG leads to the formation of agglomerated particles with irregular morphologies. Time-dependent experiments are also carried out to understand the formation process of such 3D hierarchical flower-like nanostructures. Fig. S2 (see the ESI†) shows the SEM images of samples obtained with different reaction durations. At the early stage of the reaction, 2 h, hydrolysis of $Ti(SO_4)_2$ gives rise to the formation of $TiO_2$ nuclei and the as-formed nuclei aggregate fast and react to form a hierarchical nanostructure with short 1D thorns formed on the surface. When the reaction duration is increased, these thorns with high-energy sites will then serve as nucleation centers that allow the subsequent adsorption of Ti(IV) and the crystal growth of $TiO_2$, resulting in long nanowires.

After microwave refluxing treatment, obvious morphological changes can be observed, as shown in Fig. 2c–f. For the deposition of the nanocrystals on the $TiO_2$ structures, the CdS, ZnS, ZnO, or $CeO_2$ product can be uniformly decorated on the surface of the $TiO_2$ nanoflower. Fig. 3a shows the typical TEM images of the $TiO_2$–CdS hetero-nanostructures from which it can be clearly seen that monodisperse CdS nanocrystals are tightly deposited onto the $TiO_2$ nanowires and the resultant nanohybrids well duplicate the morphology of the $TiO_2$ nanoflowers. This result is in good agreement with the SEM analysis. The EDS analysis (inset in Fig. 3a) further reveals the existence

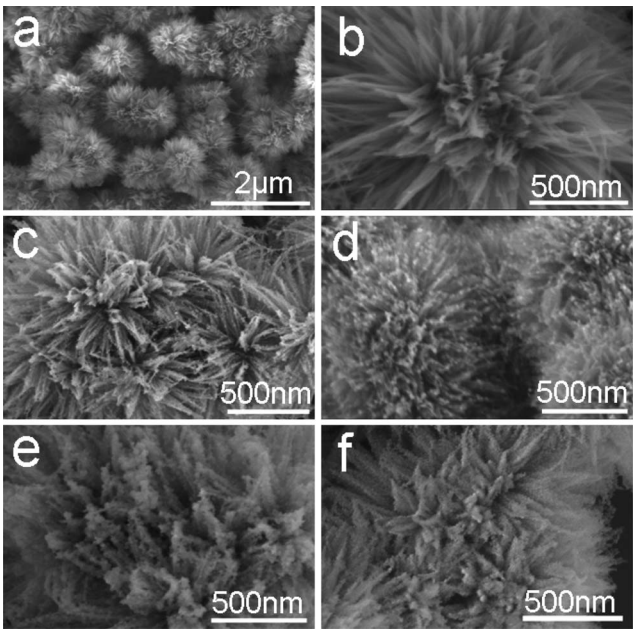


**Fig. 2** SEM images of the as-obtained hierarchical flower-like $TiO_2$ nanostructures: (a) low magnification, and (b) high magnification; SEM images of different hierarchical heterostructures obtained *via* a microwave-assisted method: (c) $TiO_2$–CdS, (b) $TiO_2$–ZnS, (e) $TiO_2$–ZnO, and (f) $TiO_2$–$CeO_2$.

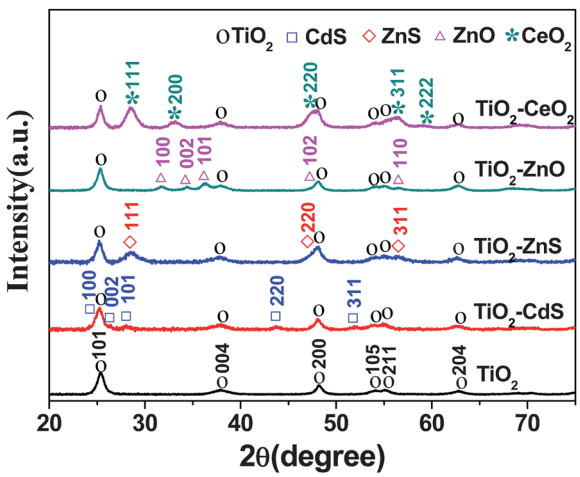


**Fig. 1** XRD patterns of the as-prepared hierarchical flower-like $TiO_2$ nanostructures and different $TiO_2$-based hetero-nanostructures.

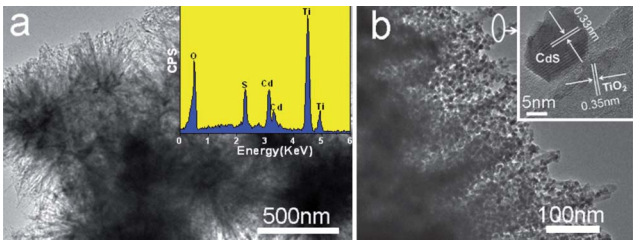


**Fig. 3** TEM images of the as-prepared $TiO_2$–CdS hetero-nanostructure: (a) low magnification, and EDS pattern (inset), (b) high magnification, and HRTEM image (inset).

of CdS nanocrystals on the $TiO_2$ nanoflower surface. The spatial distribution of the composition (Ti and Cd elements) in the foreside of a single nanoflower is further studied by elemental mapping (Fig. S3, see the ESI†). TEM and high-resolution TEM (inset) images of the foreside of a flower are shown in Fig. 3b, which also demonstrate that the CdS nanocrystals are decorated onto the $TiO_2$ framework and they are about 10 nm in diameter. Additionally, only aggregated CdS could be obtained by a similar procedure described as above without the presence of $TiO_2$ nanoflowers; the XRD pattern and SEM image are shown in Fig. S4 and S5 (see the ESI†).

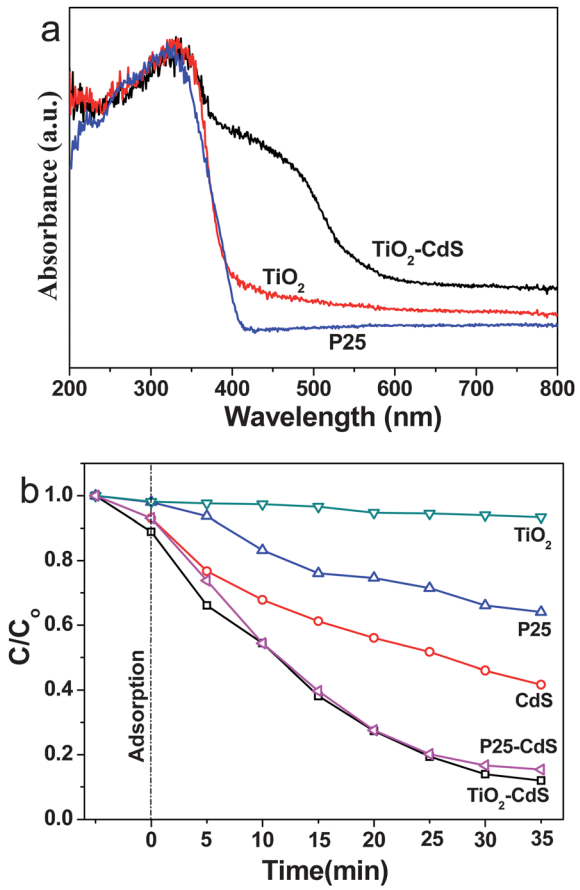


**Fig. 4** (a) UV-vis DRS spectra of the as-prepared hierarchical flower-like $TiO_2$ nanostructures, P25 and $TiO_2$–CdS hetero-nanostructure; (b) photocatalytic degradation of MO in the presence of different photocatalysts under visible-light irradiation.

Fig. 4a shows the UV-vis diffuse reflectance spectra of the as-prepared pure $TiO_2$ nanoflowers, P25 and $TiO_2$–CdS hetero-nanostructures. For pure $TiO_2$ nanoflowers, their absorption displays a characteristic UV region with a wavelength below 400 nm, which can be attributed to the intrinsic bandgap of $TiO_2$. However, $TiO_2$–CdS hetero-nanostructures exhibit significant broadened absorption covering the visible-light region because of the presence of the sulfide phase or some defects.[29] As a result, the photocatalytic activity of the as-prepared nanohybrids is improved. Fig. 4b presents the photocatalytic activities of the as-prepared $TiO_2$–CdS hierarchical heterostructures, which were evaluated for the degradation of the organic dye MO under visible-light irradiation, with the results from $TiO_2$ nanoflowers, commercial Degussa P25 nanoparticles, and pure CdS nanoparticles for comparison. $C$ is the concentration of MO after light irradiation for a certain period, and $C_o$ is the MO concentration before reaching adsorption/desorption equilibrium in the dark. After irradiation for 35 min, nearly 88.0% of MO is degraded by the $TiO_2$–CdS hetero-nanostructures, whereas other samples including P25–CdS nanocomposites, pure CdS, P25 and hierarchical flower-like $TiO_2$ nanostructures exhibit lower activities with degradation rates of about 84.6%, 58.3%, 35.9% and 6.6%, respectively. Fig. S6 (see the ESI†) shows the absorption spectra of the MO solution at different exposure times using the as-prepared $TiO_2$–CdS hetero-structures as the catalyst under visible-light irradiation. As the conduction band of CdS is more negative than that of $TiO_2$, the electrons quickly transfer to the conduction band of $TiO_2$ when CdS is excited under visible-light illumination, whereas the generated holes accumulate in the valence band of CdS. The simultaneous transfer of electrons and holes in the $TiO_2$–CdS nanohybrids system increases both the yield and the lifetime of the photogenerated carriers by separating the electron–hole pairs and reducing charge recombination in the electron-transfer process, and consequently enhances the photocatalytic performance.[30] The schematic diagram representing the charge-transfer process in the $TiO_2$–CdS hetero-nanostructures is shown in Scheme S1 (see the ESI†). We have further studied the stability and reusability of the photocatalyst by collecting and re-using the same photocatalysts for 4 cycles (Fig. S7, see the ESI†). The results show that there is some loss of photocatalytic activity during the cycle test, which might be mainly caused by photoirradiation of CdS and partly caused by the loss of the photocatalysts during each collection and rinsing step.

In summary, we have proposed an effective and general microwave-assisted strategy for the deposition of monodisperse metal sulfide/oxide nanocrystals on the surface of a 3D hierarchical flower-like nanostructure to form $TiO_2$-based metal sulfide/oxide hetero-nanostructures. This is a facile and rapid process, requiring only a low level of microwave irradiation (300 W), through which a conformal CdS, ZnS, ZnO or $CeO_2$ nanocrystal layer can be deposited onto the 3D hierarchical flower-like $TiO_2$ nanostructure, with retention of the uniformity of the original $TiO_2$ nanoflowers. As a proof-of-concept demonstration of the functional properties of these hierarchical hetero-structures, the as-prepared $TiO_2$–CdS hetero-nanostructure is investigated in-depth for the photodegradation of MO, and

obviously enhanced photocatalytic activity is observed compared with $TiO_2$ nanoflowers, P25 and pure CdS under visible-light illumination. It is believed that this facile, rapid microwave-assisted strategy is scalable and can be extended to synthesize other 3D hierarchical hetero-nanostructures for different applications.

## Acknowledgements

Y. Hu greatly acknowledges the financial support from the Natural Science Foundation of China (21171146).

## Notes and references

1 Y. F. Sun, B. Y. Qu, Q. Liu, S. Gao, Z. X. Yan, W. S. Yan, B. C. Pan, S. Q. Wei and Y. Xie, *Nanoscale*, 2012, **4**, 3761.
2 Y. Hu, X. H. Gao, L. Ye, Y. R. Wang, J. Q. Ning, S. J. Xu and X. W. Lou, *Angew. Chem., Int. Ed*, 2013, **52**, 5636.
3 W. L. Yang, L. Zhang, Y. Hu, Y. J. Zhong, H. B. Wu and X. W. Lou, *Angew. Chem., Int. Ed*, 2012, **51**, 11501.
4 W. L. Yang, Y. Liu, Y. Hu, M. J. Zhou and H. S. Qian, *J. Mater. Chem.*, 2012, **22**, 13895.
5 M. J. Zhou, X. H. Gao, Y. Hu, J. F. Chen and X. Hu, *Appl. Catal., B*, 2013, **138–139**, 1.
6 H. B. Wu, H. H. Hng and X. W. Lou, *Adv. Mater.*, 2012, **24**, 2567.
7 J. S. Chen, C. P. Chen, J. Liu, R. Xu, S. Z. Qiao and X. W. Lou, *Chem. Commun.*, 2011, **47**, 2631.
8 J. S. Chen, J. Liu, S. Z. Qiao, R. Xu and X. W. Lou, *Chem. Commun.*, 2011, **47**, 10443.
9 A. Fujishima, T. N. Rao and D. A. Tryk, *J. Photochem. Photobiol., C.*, 2000, **1**, 1.
10 H. H. Chen, C. E. Nanayakkara and V. H. Grassian, *Chem. Rev.*, 2012, **112**, 5919.
11 U. I. Gayaa and A. H. Abdullah, *J. Photochem. Photobiol., C*, 2008, **9**, 1.
12 G. S. Li, L. Wu, F. Li, P. P. Xu, D. Q. Zhang and H. X. Li, *nanoscale*, 2013, **5**, 2118.
13 H. Y. Yang, S. F. Yu, S. P. Lau, X. W. Zhang, D. D. Sun and G. Jun, *Small*, 2009, **5**, 2260.
14 S. L. Wang, H. H. Qian, Y. Hu, W. Dai, Y. J. Zhong, J. F. Chen and X. Hu, *Dalton Trans.*, 2013, **42**, 1122.
15 X. C. Wang, J. C. Yu, H. Y. Yip, L. Wu, P. K. Wong and S. Y. Lai, *Chem.–Eur. J.*, 2005, **11**, 2997.
16 K. Woan, G. Pyrgiotakis and W. Sigmund, *Adv. Mater.*, 2009, **21**, 2233.
17 L. L. Tan, S. P. Chai and A. R. Mohamed, *ChemSusChem*, 2012, **5**, 1868.
18 Z. Y. Zhang, C. L. Shao, X. H. Li, Y. Y. Sun, M. Y. Zhang, J. B. Mu, P. Zhang, Z. C. Guo and Y. C. Liu, *Nanoscale*, 2013, **5**, 606.
19 F. X. Xiao, *ACS Appl. Mater. Interfaces*, 2012, **4**, 7055.
20 J. S. Chen, Y. L. Tan, C. M. Li, Y. L. Cheah, D. Luan, S. Madhavi, F. Y. C. Boey, L. A. Archer and X. W. Lou, *J. Am. Chem. Soc.*, 2010, **132**, 6124.
21 H. W. Bai, Z. Y. Liu, S. S. Lee and D. D. Sun, *Appl. Catal., A*, 2012, **447–448**, 193.
22 T. J. Athauda, J. G. Neff, L. Sutherlin, U. Butt and R. R. Ozer, *ACS Appl. Mater. Interfaces*, 2012, **4**, 6917.
23 Z. K. Zheng, B. B. Huang, X. Y. Qin, X. Y. Zhang and Y. Dai, *Chem.–Eur. J.*, 2010, **16**, 11266.
24 J. Zhu, S. H. Wang, J. G. Wang, D. Q. Zhang and H. X. Li, *Appl. Catal., B*, 2011, **102**, 120.
25 G. H. Tian, Y. J. Chen, W. Zhou, K. Pan, C. G. Tian, X.-R. Huang and H. G. Fu, *CrystEngComm*, 2011, **13**, 2994.
26 S. F. Xie, B. J. Zheng, Q. Kuang, X. Wang, Z. X. Xie and L. S. Zheng, *CrystEngComm*, 2012, **14**, 7715.
27 X. L. Tana, M. Fang, J. X. Li, Y. Lu and X. K. Wang, *J. Hazard. Mater.*, 2009, **168**, 458.
28 Y. Hu, Y. Liu, H. S. Qian, Z. Q. Li and J. F. Chen, *Langmuir*, 2010, **26**, 18570.
29 S. J. Ding, X. Yin, X. J. Lu, Y. M. Wang, F. Q. Huang and D. Y. Wan, *ACS Appl. Mater. Interfaces*, 2012, **4**, 306.
30 Y. Hu, H. H. Qian, Y. Liu, G. H. Du, F. M. Zhang, L. B. Wang and X. Hu, *CrystEngComm*, 2011, **13**, 3438.

 